bExperimental and discrete element numerical analysis of side slope instability induced by fissure water underlying impervious bed

LIU Bingshan[1], LI Shihai[1], ZHANG Lei[1,2] & WANG Jianguo[3]

1. Institute of Mechanics, Chinese Academy of Sciences, Beijing 100080, China;
2. Graduate School, Chinese Academy of Sciences, Beijing 100060, China;
3. Tropical Marine Science Institute, National University of Singapore, 10 Kent Ridge Crescent, Singapore 119260

Correspondence should be addressed to Li Shihai (email: shli@imech.ac.cn)

Abstract   When the sliding mass contains impervious bed, rainfall can infiltrate into mountain via crevices and form higher artesian aquifer at impervious bed inferior. This will decrease slip resistance and increase sliding forces of the sliding mass, thus lowering the safety factor, and inducing landslide disasters. In this paper, a landslide experimental apparatus is designed for experimental studies on the mechanism of this type of landslides. Meanwhile, the non-dimensional parameters in the model experiment are taken into account using dimensional analysis. The experimental results show that (1) the ratio of the cleft water pressure to the overlying pressure is a crucial parameter affecting the stability of the slope; (2) when the shut-in pressure reaches 80% of the normal component of the pressure on the slip surface made up of rock and soil, landslide will occur; (3) the whole slope will start to slide when the shut-in pressure is equal to the normal component of the pressure formed by the overlying rock and soil on the upper 30% area. In this article, a discrete element method simulation is used to investigate the influence of cleft water pressure and shearing strength on the landslide stability. It can be concluded that the critical value of C_{cr}, φ_{cr}, which determines the slide mass stability, increases with the increase of the water pressure; if the water pressure reaches a high level, the stability of the slide mass depends mainly on C, while the influence of φ becomes smaller than C.

1   Introduction

The *in situ* observations and analysis on the landslide events indicate that water is one of the key factors which induce landslide of the mountain mass[1−8]. The mechanism of

fissure water inducing landslide can be generalized into three aspects: (1) the softening influence of water weakens the strength of materials on the slip surface[9−11]; (2) the cleft water pressure towards the slide slope free face increases sliding force[12−15]; (3) water pressure on the slip surface lowers the effective stress, thus decreasing the shear strength. Case record and brief examination indicate that the three aspects may simultaneously exist in a landslide[4,16,17], but it is quite difficult to identify the influence of single factor among them. The incorporation of conventional crevice seepage equation and general analytical procedure of slope stability is a new way to study the slope stability, for instance, adding water pressure in the limit equilibrium method[18−20]. Ones also coupled crevice network seepage model and discrete element method[21,22] to analyze the stability of water filled rock slope in engineering cases[4,23,24]. In addition, Jiao et al.[25] systematically studied how to simulate the groundwater using discrete element method, and illustrated a simple example with several block elements. The authors fore-mentioned studied the influences of water on slope stability by engineering monitoring, numerical simulation and experimental study etc. respectively. The interaction mechanism of water has three aspects as mentioned above, but up to now no one studied which one plays the dominant role in the instability of the whole slope systemically by combining experiment and numerical simulation.

Both the present modes of fissure water and the physical and mechanical characteristics of the potential slip surface are the important factors inducing landslide[9,11,18,25,26]. Iverson et al.[27] indicated that initial porosity has decisive effect on the sliding velocity of landslide. If the initial porosity of soil mass is greater than certain value, the slope will become instable once reaching a certain level. But they did not point out that concrete scope of pore pressure, furthermore, impacts the slope stability with changing the pore pressure when the slope damages. Asch et al.[10] indicated that most shallow landslides (5−20 m) are induced by the pore pressure on the slip surface, especially when the sliding mass contains argillaceous impervious bed. Owing to the low penetrability of the clay band, groundwater or rainfall can form high shut-in pressure after it permeates into the underside of the impervious bed via crevices. This will reduce the effective normal stress and slide resistance, meanwhile the sliding force does not depress, so the probability that slope loses its stability increases greatly. Harr[28] found that rainfall could bring out transient saturation on the interface between soil mass and subsoil by experiment observation, because the size distribution of pore transfers greatly near the interface. This makes the transmissibility of soil decrease, prevents water infiltrating further, so high pressure develops near the interface, then the stability of landslide mass will depress. Slope will be in a critical state if the pore pressure makes the sliding force balance to the slip resistance; if the sliding force is greater than the slip resistance, slope will begin sliding failure.

The present experimental apparatus can only simulate the slopes whose inclination angle is relatively large[27]. The pore pressure supplied by the apparatus is not enough to

make the slope lose its stability. For example, the dip of bedrock in the experiments carried by Iverson[27] is 31°, and landslide would not occur if the porosity is ≤0.39±0.03. In fact, the dip of quite a few landslides is quite small; for example, the average dip of Maoping landslide on the Qing River in Hubei Province is only 15°. Additionally, it is difficult to identify the three aspects of water action mechanism completely due to the limitation of the physical experiment condition. Therefore, numerical simulation is a good complement tool to study the mechanism.

In this article, we studied the stability of a slope containing an impermeable bed through three ways: model, dimensional analysis and discrete element method. Then the quantitative relationship between the ratio of the pore pressure to burden pressure and the landslide induce has been obtained. The influences of cleft water pressure on the stability of a slope, whose dip was 18°, were studied by experiment apparatus designed by the authors, which could simulate those landslides whose dip were quite small. A law of the critical C and φ values varying with different water pressures is derived by the discrete element method simulation. Moreover, back analysis for critical C_{cr} and φ_{cr} of the watered slip surface gave out the safe scope of the model subject to different water pressures.

2   Experimental apparatus and operational principle

The slope in Fig. 1, which contains an impermeable layer, is simplified to a mechanical model shown in Fig. 2. The general layout of the experimental apparatus and its operational principle are shown in Fig. 3. The test kit is 1.5 m long, 1.1 m wide and 0.05 m thick。It has ten self-contained units along the long side that are marked as 1 to 10 from right down to left upper. Each unit has water intake set and piezometric tube, respectively. The piezometric tube is fixed in the middle of the unit, so the pressure measured with the piezometric tube can be taken as the average water pressure in the unit, and it is the average pore water pressure over the corresponding unit. The water intake set is composed of storage box, water inlet box and water inlet tube. Storage box and water inlet box can keep the input pressure constant. The water pressure in the unit can be changed by adjusting the valve of the water inlet box or the water height in the storage box and water inlet box. The slip surface is simulated with 0.02 m thick clay layer that can be watered from the units. Bedding course is paved tightly with granite blocks,
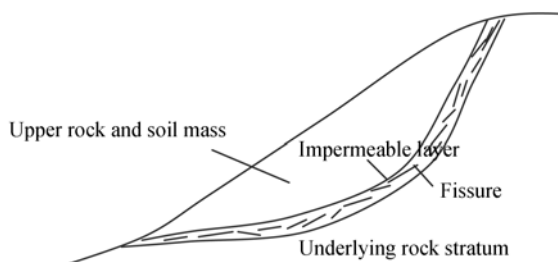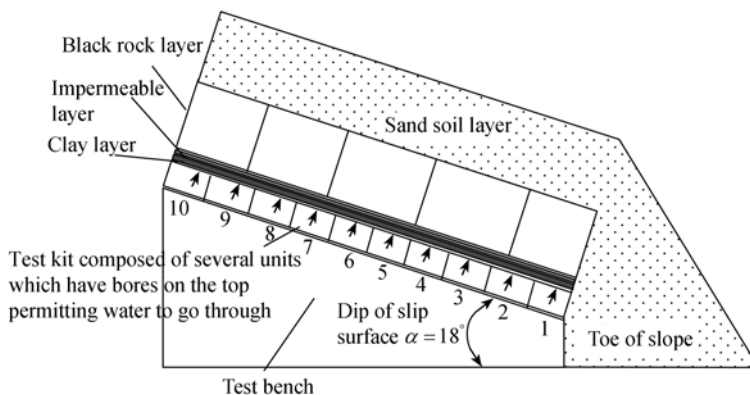

Fig. 1.   Geologic profile.
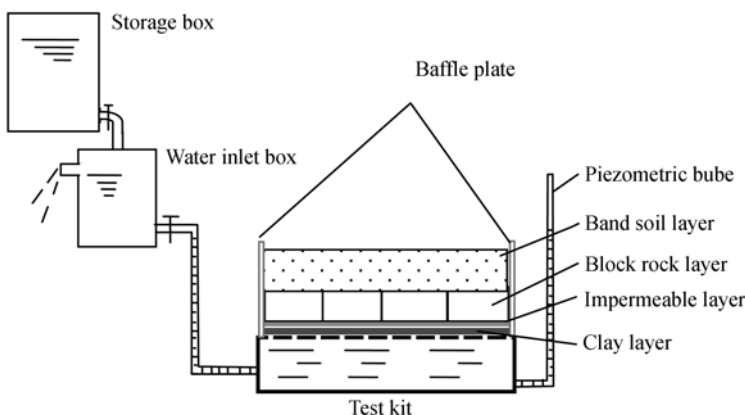
Fig. 2.   Mechanical modal.

Fig. 3.   Schematic figure of the experiment apparatus.

and it is on the upper of the clay layer. The impervious bed is simulated by paving a layer of plastic foil between the clay layer and the granite block layer. The upper of the block layer is sand soil layer. Both the block layer and sand soil layer are 0.1 m thick.

The experimental apparatus has the following features:

(1) It can measure the pore water pressure on slip surface at any moment.

(2) It can conveniently simulate landslides with different dips by adjusting the input pressure and the angle of the test kit laid.

(3) One or several units can be watered respectively to consider the heterogeneous distribution of the confined water in the slope.

3   Control parameters in experiment and the dimensional analysis

According to Fig. 2, the parameters affecting the slope stability include: (1) Geometric parameters: the dip angle of sliding surface α; the thickness of block rock layer t_1; the thickness of sand soil layer t_2; the length of slope along the sliding surface l and the

width b. (2) Physical parameters: The effective cohesion c' and effective angle of internal friction ϕ' of the clay layer; the rock density ρ_1 and the density ρ_2 of the sandy soil; acceleration of gravity g; pore water pressure p. (3) Boundary conditions: the slip resistant shear force F'_s acting on the slope by the toe. Both sides of the slope are baffle plates, and the frictional coefficient f is considered to be a constant during slope deform and slide.

The following dimensionless quantities are composed of the parameters mentioned above:

$$\alpha, \quad \phi', \quad f, \quad \frac{t_2}{t_1}, \quad \frac{l}{t_1}, \quad \frac{b}{t_1}, \quad \frac{\rho_2}{\rho_1}, \quad \frac{p}{\rho_1 g t_1}, \quad \frac{c'}{\rho_1 g t_1}, \quad \frac{F'_s}{\rho_1 g t_1}.$$

If F_τ and F_σ are the tangential force and normal force on the slip surface, respectively,

$$\frac{F_\tau}{\rho_1 g t_1} = f\left(\alpha, f, \frac{t_2}{t_1}, \frac{b}{t_1}, \frac{l}{t_1}, \frac{\rho_2}{\rho_1}\right), \tag{1}$$

$$\frac{F_\sigma}{\rho_1 g t_1} = f'\left(\alpha, f, \frac{t_2}{t_1}, \frac{b}{t_1}, \frac{l}{t_1}, \frac{\rho_2}{\rho_1}, \frac{p}{\rho_1 g t_1}\right). \tag{2}$$

As $F_\tau - F_\sigma tg\phi' - c' - F'_s > 0$, the whole slope will start to slide. Considering the soil at the toe of the slop has little resistant force after saturated, the condition that the whole slope slides is $F_\tau - F_\sigma tg\phi' - c' > 0$.

Assuming the safety factor of the slope is k, then

$$k = \frac{F_\tau}{F_\sigma tg\phi' + c'} = f\left(\alpha, \phi', f, \frac{t_2}{t_1}, \frac{b}{t_1}, \frac{l}{t_1}, \frac{\rho_2}{\rho_1}, \frac{p}{\rho_1 g t_1}, \frac{c'}{\rho_1 g t_1}\right), \tag{3}$$

where l, b, t_1, t_2, ρ_1 and ρ_2 are constants in the experiment, respectively. Select the normal stress on the slip surface formed by the block rock layer and the sand soil layer as variable, then

$$k = f\left(\alpha, \phi', \frac{p}{(\rho_1 g t_1 + \rho_2 g t_2)\cos\alpha}, \frac{c'}{(\rho_1 g t_1 + \rho_2 g t_2)\cos\alpha}\right)$$

$$= f\left(\alpha, \phi', \frac{p}{\sigma}, \frac{c'}{\sigma}\right), \tag{4}$$

where $\sigma = (\rho_1 t_1 + \rho_2 t_2)\cos\alpha$ indicates the normal stress on the slip surface yielded by the overlying rock and soil.

From formula (4), we found that the slope stability depends on the slope angle α, the ratio of the cleft water pressure to the normal stress of the slip surface yielded by the overlying rock and soil p/σ, the internal friction angle φ' and the ratio of cohesion to the normal stress yielded by the overlying rock and soil c'/σ. In the experiment, $\alpha = 18°$; $t_1 = t_2 = 0.1$ m; $\rho_1 = 2.7 \times 10^3$ kg/m³; $\rho_2 = 1.7 \times 10^3$ kg/m³. The angle of slope is fixed according to the concrete condition of the experiment. φ' and c' can be thought as constant, because the slope is dunked sufficiently. Thereby, the slope stability only depends on p/σ in the experiment.

4 Experimental results and analysis

4.1 The relationship between the slope stability and the cleft water pressure

The experiment was carried out from 1—8 units for the operation convenience. During the experiment, the test kit was watered in advance and kept the pressure at about 0.1 m water column. The clay layer was dunked for 3—4 h to make it saturate enough. Then increase water pressure in all of the units step by step, after the deformation of the rock and soil aggregate tending to stability, increase the water pressure again, keeping the interval not less than 20 min. The values were recorded before and after changing the pressures up to the slope sliding. The experimental results are listed in Table 1.

Table 1   Experimental result when all the units were watered simultaneously

Experimental order	Water pressure in the unit (cm water column)								Average pressure (cm water column)
	Sequence number of the units								
	1	2	3	4	5	6	7	8	
1	28	30	32	33	37	34	35	29	32.3
2	33	34	28	30	32	30	33	27	30.9
3	31.5	34	35	33.5	34	32	28.5	30.5	32.4
4	33	35	34	36	33	30	28	31	32.5
5	31	30	29	33	30	33	34	30	31.3

Suppose the pressure on the slip surface distributing evenly, the normal stress on the slip surface formed by the overlying rock and soil aggregate can be illustrated as (water column):

$$\sigma = \frac{(\rho_1 t_1 + \rho_1 t_2)\cos\alpha}{\rho_w}, \tag{5}$$

where, ρ_1 and ρ_2 are the densities, and t_1 and t_2 are the thickness of block rock layer and sand soil layer respectively, α is the slope angle. The average normal stress can be given after the experimental parameters substituted into formula (5). The relationship between the critical pore-water pressure and the normal stress yielded by the overlying rock and soil is illustrated in Table 2.

Table 2   The relationship between the critical pore-water pressure and the normal stress yielded by the overlying rock and soil

Sequence number of the experiment	1	2	3	4	5
Critical pore-water pressure p (cm water column)	32.3	30.9	32.4	32.5	31.3
Normal stress yielded by the overlying rock and soil σ (cm water column)			39.5		
Ratio p/σ (%)	81.7	78.2	82.0	82.3	79.2

From Table 2, we find that the slope will lose its stability when the ratio between the pore-water pressure and the normal stress on slip surface yielded by the overlying rock and soil reaches about 80%.

4.2   The relationship between slope stability and the area watered

Plenty of rainfall can form high shut-in pressure after it permeates to underside of the impervious bed following crevices. As the pressure of confined water is equivalent to the weight of overlying rock and soil and the holding area is more than some percentage of the whole area of slip surface, the slope would slide impelled. The test kit was watered from the top keeping the pressure nearly the normal stress yielded by the overlying rock and soil, then to increase the number of units till the slope sliding. In order to simulate process conveniently, the pressures of No. 9 and No. 8 units were adjusted to 0.4 m water column first and retained for 20 min. Then adjust the pressure of units in descending order until the slope slid. The interval was 20 min. All the slopes slid wholly because the units were watered from the top of the test kit.

Table 3   The number of units watered when the slope slid

Sequence number of the experiment	1	2	3	4	5	6
The number of units watered when the slope slid	6	4	4	3	3	3
The area watered/the whole area (%)	66.7	44.4	44.4	33.3	33.3	33.3

The normal stress on the slip surface yielded by the overlying rock and soil aggregate was balanced with the pore-water pressure when the pressure in the unit reached 0.4 water column. From the experimental result in Table 3, we found that the slope started sliding when 33.3% of the area was in the state.

5   Numerical simulation with three-dimensional rigid block discrete element method

The strength of rock and soil aggregate is difficult to identify in engineering practice, even though in laboratory test. Laboratory test cannot completely embody the influence of rock mass structure for the limit of the scale and frequency of it. But numerical simulation can identify the mechanical parameters of the rock mass by inverse analysis, and investigate the influence of the complex structure of rock mass. Thereby, it can complement the limitation of laboratory test, and can improve the apprehension to the mechanism of landslide. The face-face contacted three-dimensional discrete element method was adopted in numerical simulation, which is developed by the Institute of Mechanics,

the Chinese Academy of Sciences. Suppose there are three groups of main joint planes in this model. These joint planes divide the scope into a set of parallelepiped elements. There are four Lump points in every surface (the black points shown in Fig. 4). The force acted on the face is equivalent to four forces on the LP points by static equilibrium. The element can embed in another one on the contacted surface, although the elements are rigid. It can be thought that there are imagined tangential and normal springs on the contacted surface (see Fig. 9 below in sec. 5.3), and the deformation of the element and joint is reflected through this method. The mutual forces acted among the elements are transferred by the imagined springs. Water pressure should be exerted on the LP points when there is water in the crevices. The motion of the elements must satisfy the law of inertia. The explicit dynamic relaxation method [28] is adopted in the process of solution. Select three groups of the main joint planes and assign values for their C, φ, elastic modulus and stiffness, etc. according to the engineering practices. The block discrete element method can completely illustrate the influence of the structure, such as joint planes etc., on the slope stability, so it has been applied in the analysis of slope stability[15,29,30].
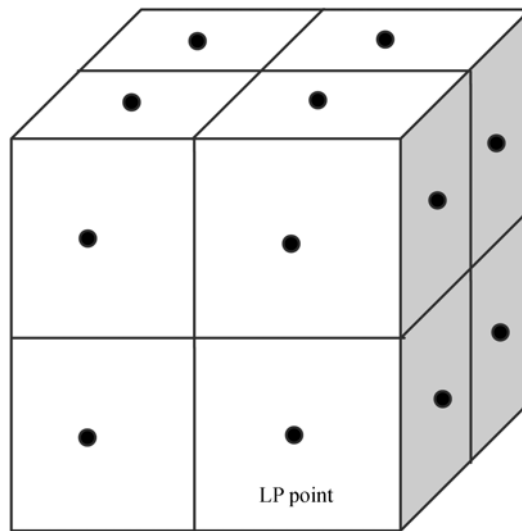

Fig. 4.   Rigid block element.

5.1   The material parameters and the boundary conditions

The calculating domain in numerical simulation is as same as the experimental dimension. The dimension of maximum scope of research is 1.35 m×0.9 m×0.3 m. The toe of the slope was neglected in the simulation because its strength decreased greatly for the dunking. According to the paving of the granite blocks, select the physical dimension of the granite block as the dimension of the element, which is 0.2 m×0.1 m×0.1 m. The whole study domain was divided into 189 elements distributed into 7×9×3 at the directions of x, y and z, respectively, as shown in Fig. 5. The slope angle is 18º, and the bot-

tom layer is fixed in all freedoms with the other boundaries being free. The physical mechanical parameters of the sand soil and granite blocks are listed in Table 4.
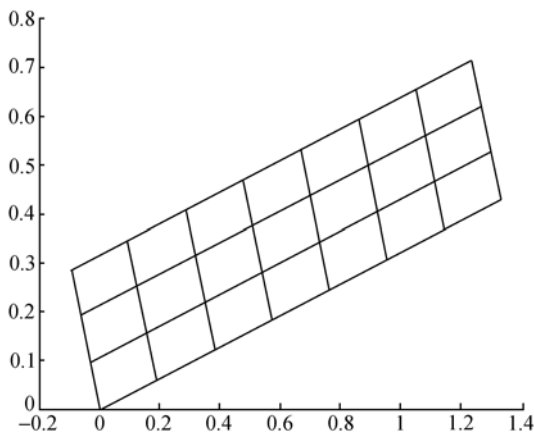

Fig. 5.   The state before sliding.

Table 4   Geometry and mechanical parameters of the soil mass, granite blocks and joints

	Density (kg/m^3)	Poisson's ratio	Elastic modulus (N/m^2)	Normal stiffness (N/m^3)	Tangential stiffness (N/m^3)
Soil mass	1.7×10^3	0.3	2.0×10^9	2.0×10^{11}	1.5×10^{11}
Granite block	2.7×10^3	0.2	2.0×10^{10}	5.0×10^{11}	2.5×10^{11}
			Angle of internal friction φ(°)	Cohesion C (pa)	
Between the soil elements			27	2000	
Between the rock elements			37	3000	
Between the rock and soil elements			25	1000	
Appellations of the structural surfaces	Geometry description	The angle from x axis	The angle from y axis	The angle from z axis	Space
J_1	Normal to the bedrock surface	0°	90°	72°	0.2 m
J_2	Normal to the slip surface and parallel to xoz face	90°	0°	90°	0.1 m
J_3	Parallel to bedrock surface	180°	90°	18°	0.1 m

5.2   Numerical simulation using the three-dimensional discrete element method and the results of inverse analysis

The C and φ values of the slip surface were identified by inverse analysis for five different operating conditions, which were $h_w = 0$ m, $h_w = 0.15$ m, $h_w = 0.32$ m, $h_w = 0.4$ m and $h_w = 0.4$ m while only 43% area upper the slope was watered. The material and geometry parameters were kept constant in the simulation. For a given C, φ is changed so as to find the critical angle of internal friction-φ_{cr}. Furthermore, for another given C, the above process was repeated. If giving a value of φ, the critical value of cohesion-C_{cr} can be found out by the same way. The state of slope after sliding is shown in Fig. 6. The critical curves calculated are illustrated in Fig. 7, in which the

y-axis indicates the ratio of the critical cohesion versus the overlying pressure and the *x*-axis indicates the critical angle of internal friction. We can get the following rules from Fig. 7.
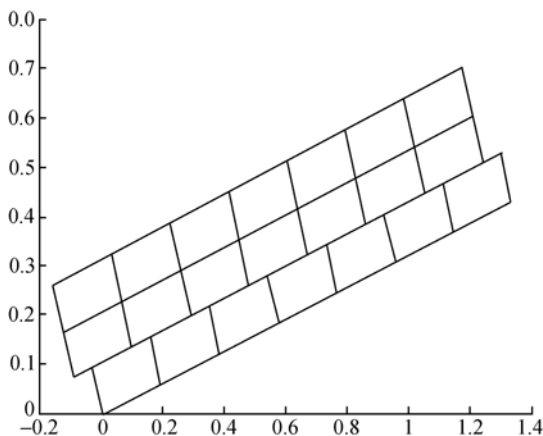

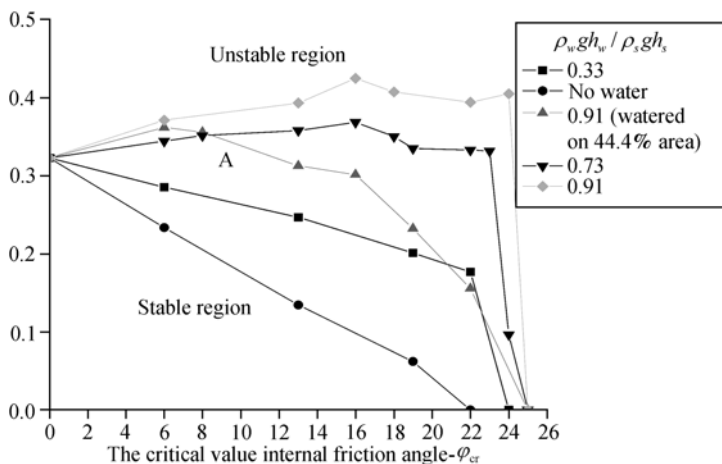Fig. 6.   The state after sliding.

Fig. 7.   The relationship of the dimensionless quantity-$C_{cr}/\rho_s g h_s$ and φ_{cr}.

(i) The inverse analysis for the strength parameters of the slip surface.   The slope stability under two operating conditions were studied, which are watering on the whole slip surface and watering on part area upper the slip surface. The values of C and φ under the two conditions are equal because the slip surface are saturated enough. So the intersection point A of the curve of $h_w = 0.32$ m ($\rho_w g h_w / \rho_s g h_s = 0.73$, watering wholly) and the curve of $h_w = 0.4$ m ($\rho_w g h_w / \rho_s g h_s = 0.91$, watering on 43% area partly) is the point wanted. We can find that $\varphi = 8.5°$ and $C = 1500$ Pa corresponding to point A in Fig. 7. To the saturated clay, φ usually is from 0° to 10° and C is about 2000 Pa according to the engineering practice. So the reverse analysis results are identical to the experimental

results on the whole.

(ii) The results identified with the limit equilibrium method.

(1) The critical angle of internal friction-φ_{cr} increases almost linearly with the critical cohesion-C_{cr} without watering.

(2) The basic trend when the artesian head is low relatively is as the same as without watering. But it needs a higher value of C to maintain the stability.

(3) With the increase of artesian head, the values of C_{cr} and φ_{cr} determining the stability of slope increase, and the instable zone within the curve extends outwards as well.

(iii) The effect of the structure of rock mass

(1) The effect of the structure of rock mass on the whole stability. The result given by the limit equilibrium method usually is considered having bias towards more safe. But in the experiment without watering and $C = 0$, the critical angle of internal friction obtained by the limit equilibrium method is 18º, while 22º given by the discrete element method which is more identical to the experimental result. That is to say, the slope considered stable by the limit equilibrium method might be instable by the discrete element method. The difference mainly attributes to the structure of rock mass. The limit equilibrium method thinks that every part of the slope reaches its maximum strength at the same time and slides along the slip surface certainly neglecting the structure of rock mass normal to the slip surface no matter how complex it is. But there are lots of constructional surfaces in rock mass such as joints, cleavages and crevices, etc., and this has significant influence on the deformation of the sliding mass. So it is difficult for every part of the slop to reach its maximum strength at the same time. It is reasonable for the critical φ_{cr} to be higher than that given by the limit equilibrium method to maintain the slope stability after considering the influences of heterogeneity of the stress distribution in parts of the slope and structure of rock mass. Thus the discrete element method is more reasonable than the limit equilibrium method at the aspect of considering the structure of rock mass.

(2) The effect of reduction of total stress on the contacted surface in some zones. The critical curve runs up if the water pressure is high relatively, although it is much slow. This is different from the result gotten by the limit equilibrium method. The result given by the discrete element method shows that the stress distribution illustrated in Fig. 8 is uneven in the slope toe. The y-axis in the figure indicates the ratio between the normal stress on slip surface and the upper pressure. The total stress decreases because the average stress decreases with the increasing of φ, so a higher value of C is needed to keep the slope stable.

(3) The effect of heterogeneity of the stress distribution on slip surface. In the case calculated, the slope can keep stable when the value of φ is larger than 25°, even though the value of C is very small. This is not identical to the result given by the limit equilibrium method[16,17]. In fact, the water pressure on slip surface is supposed to act evenly on
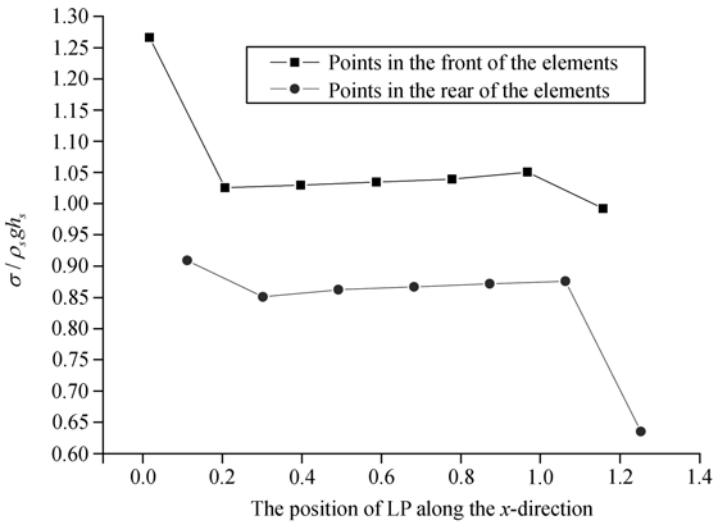
Fig. 8.   The distribution of normal stress on slip surface when $h_w = 0.32$ m or $\rho_w g h_w / \rho_s g h_s = 0.73$.

slices in the limit equilibrium method, so it is unable to keep the slope stable under any value of φ if the water pressure is equal to or higher than the overlying pressure and C is equal to zero. The block element in the discrete element method is allowed to rotate, so it is possible that there is high compressive pressure acting on the under part of a block while the upper has a crack illustrated in Fig. 9. The pressure can yield large resistance. That is to say, the stress acting on a block distributes unevenly, and the heterogeneity may increase the resistance.
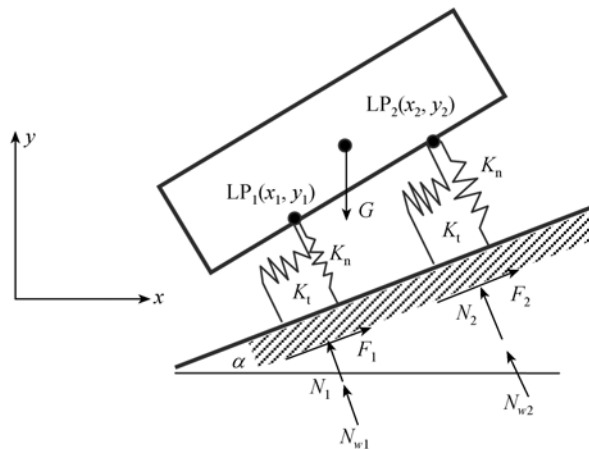

Fig. 9.   The sketch of a block on the slip surface.

5.3   The simplified analysis using the discrete element method simulation

Select a block element on slip surface as the objective to investigate the difference between the limit equilibrium method and the discrete element method. The question can

be simplified into two-dimension along the slip surface illustrated in Fig. 9, because the load does not vary along the width. The forces acting on the element are gravity-G, bearing force-N_1 yielded by the slip surface and water pressure-N_{w1} acted on the first LP point, bearing force-N_2 yielded by the slip surface and water pressure-N_{w2} acted on the second LP point. In fact, N_1 and N_2 are the effective normal stress on the slip surface, they decrease with the increase of water pressure。 Suppose the length is L and the height is h. Under small deformation, the equilibrium equations along the tangential and normal directions of the slip surface are:

$$F_1 + F_2 - G\sin\alpha = 0 , \tag{6}$$

$$N_1 + N_2 + N_{w1} + N_{w2} - G\cos\alpha = 0, \tag{7}$$

$$(-N_1 - N_{w1} + N_2 + N_{w2})\frac{L}{4} + (F_1 + F_2)\frac{h}{2} = 0 . \tag{8}$$

Substituting (6) into (8) and combining with (7), N_1 is obtained as

$$N_1 = G\left(\frac{\cos a}{2} + \frac{h}{L}\sin a\right) - N_{w1}. \tag{9}$$

Substituting it in (7), then

$$N_2 = G\left(\frac{\cos a}{2} - \frac{h}{L}\sin a\right) - N_{w2}. \tag{10}$$

Suppose the water pressure on the slip surface is even, then $N_{w1} = N_{w2}$.

Thus, $N_1 > N_2$,

and $N_1 - N_2 = 2G\frac{h}{L}\sin\alpha. \tag{11}$

This shows that the stress on the slip surface is uneven, even though it is simple as this. It is illustrated in Fig.8 that the normal stress on the slip surface distributes unevenly. The counting parameters are assigned as follows: $h_w = 0.32$ m, $\varphi = 13°$ and $C = 1500$ Pa. The vertical axis indicates the ratio between the stress-σ on LP point and the overlying pressure-$\rho_s g h_s$, and the horizontal axis indicates the position of the LP point along x-direction. It can be seen from the figure that the stresses on different LP points have great difference, the maximum is almost two times than the minimum. This gives the reason why the value of φ_{cr} differs greatly with that gotten by the limit equilibrium method if C is equal to zero.

Suppose the contact length between the element and slip surface is L, then according to the Mohr -Coulomb criterion with effective stress, the condition keeping the slop stable is:

$$CL + (N_1 + N_2)tg\varphi \geqslant G\sin\alpha.$$

That is

$$CL + \left(G\cos\alpha - N_{w1} - N_{w2}\right)tg\varphi \geqslant G\sin\alpha. \tag{12}$$

Analyze the result according to it, then

(1) As a whole, the effective normal stress, $G\cos\alpha - N_{w1} - N_{w2}$, decrease for the existing of water pressure, so it needs higher values of C_{cr} and φ_{cr} to maintain the stability of slope.

(2) When water pressure is low, the bottom surface of the element keeps contact with the slip surface on the whole length, so CL and $G\cos\alpha - N_{w1} - N_{w2}$ are constant under a same water pressure. As a result, the critical value of C keeping the slope stable decrease with the increase of the value of φ.

(3) As water pressure reaches a specific degree, $G\cos\alpha - N_{w1} - N_{w2}$ becomes small, so the effect of φ is very little, and the slope stability mainly depends on the value of C.

(4) When the water pressure increase further, LP_2 point of the element departs form the slip surface, N_2 is equal to zero or becomes pulling force, the friction force $f_2 = 0$, so the resistance is supplied by LP_1 point only. Now, $N_1 = G\cos\alpha - N_{w1} - N_{w2}$, but the contact length decreases from L to $L' = L/2$, then the condition that keep the slope stable becomes:

$$CL' + \left(G\cos\alpha - N_{w1} - N_{w2}\right)tg\varphi \geqslant G\sin\alpha. \tag{13}$$

Because the contact length decreases, both C and φ must increase to maintain the slope stable when the value of φ is low. The critical value of C decreases after φ reaches certain degree.

6 Conclusions

In the article, the mechanism of landslide for slopes containing a impervious bed is investigated by both a landslide experimental apparatus we developed and by the discrete element method simulation. The results include as follows:

(1) If the whole slip surface is watered, the sliding mass in the model experiment will lose it's stability when the ratio between the pore-water pressure and the normal stress on slip surface yielded by the upper rock and soil reaches about 80%.

(2) If the upper of the slip surface is partly watered, the slope starts sliding when the normal stress on the slip surface yielded by the overlying rock and soil aggregate is balanced with the pore-water pressure on about 33.3% area of the slip surface.

(3) It can be found, by numerical simulation, that the values of C_{cr} and φ_{cr} determin-

ing the stability of slope increase with the increasing of artesian head. When water pressure reaches a specific degree, the effect of φ is very little, the slope stability depends mainly on the value of C.

(4) The values of C and φ can be identified by inverse analysis according to different operating conditions. The results given by the discrete element method is more reasonable than by the limit equilibrium method, since the former incorporates the structure of rock mass and the heterogeneity of the stress distribution on slip surface.

Although the discrete element method take many factors affecting the slope stability into account, the reliability must be validated further in engineering practices. In the article, because the model is largely simplified to study the mechanism of pore-water pressure affecting the slope stability, it has some certain difference from the actual operating condition.

References

1. Lan, H. X., Zhou, C. H., Lee, C. F. et al., Rainfall-induced landslide stability analysis in response to transient pore pressure–A case study of natural terrain landslide in Hong Kong, Science in China, Series E, 2004, 46 (Suppl): 52－68.
2. Braathen, A., Blikra, L. H., Berg, S. S. et al., Rock-slope failure in Norway; type, geometry, deformation mechanisms and stability, Norwegian J. of Geology, 2004, 84(1): 67－88.
3. Garinger, B., Alfaro, M., Graham, J. et al., Instability of dykes at Seven Sisters Generating Station, Canadian Geotechnical Journal, 2004, 41: 959－971.
4. Cappa, F., Guglielmi, Y., Soukatchoff, V. M. et al., Hydromechanical modeling of a large moving rock slope inferred from slope leveling coupled to spring long-term hydrochemical monitoring: example of the La Clapiere landslide (Southern Alps, France), J. of Hydrology, 2004, 291: 67－90.
5. Mikos, M., Cetina, M., Brilly, M., Hydrologic conditions responsible for triggering the Stoze landslide, Slovenia. Engineering Geology, 2004, 73: 193－213.
6. Nichol, D., Graham, J. R., Remediation and monitoring of a highway across an active landslide at Trevor, North Wales. Engineering Geology, 2001, 59: 337－348.
7. Sah, M. P., Mazari, R. K., Anthropogenically accelerated mass movement, Kulu Valley, Himachal Pradesh, India. Geomorphology, 1998, 26: 123－138.
8. Terlien, M. T. J., Hydrological landslide triggering in ash-covered slopes of Manizales (Colombia), Geomorphology, 1997, 20: 165－175.
9. Orense, R., Farooq, K., Towhata, I., Deformation behavior of sandy slopes during rainwater infiltration, Soils and Foundations, 2004, 44(2): 15－30.
10. Van Asch Th, W. J., Buma, J., Van Beek, L. P. H., A view on some hydrological triggering systems in landslides, Geomorphology, 1999, 30: 25－32.
11. Wang, J. G., Investigation on the method of middle and short prognosis of landslides, J. of Chongqing University, 1991, 14(3): 67－72.
12. Gallardo, A. L. C. F., Saqnchez, L. E., Follow-up of a road building scheme in a fragile environment, Environmental Impact Assessment Review, 2004, 24: 47－58.
13. Tsaparas, I., Rahardjo, H., Toll, D. G. et al., Controlling parameters for rainfall-induced landslides, Computers and Geotechnics, 2002, 29: 1－27.
14. Xie, M., Esaki, T., Cai, M., A time-space based approach for mapping rainfall-induced shallow landslide hazard, Environmental Geology, 2004, 46: 840－850.

15.   Yan Lin, Li Shihai, Dong Dapeng et al., The discrete element numerical simulation for Wulong landslide, Mechanics and Practice, 2002, 24(suppl.): 94—99.

16.   Collins, B. D., Znidarcic, D., Stability analyses of rainfall induced landslides, J. of Geotechnical and Geoenvironmental Engineering, ASCE, 2004, 130(4): 362—372.

17.   Okura, Y., Kitahara, H., Ochiai, H. et al., Landslide fluidization process by flume experiments, Engineering Geology, 2002, 66: 65—78.

18.   Cheng, H. K., Ai, N. S., The basic characteristics and effects of the groundwater pressure in rock slope, Journal of Lanzhou University (Natural Science Edition), 1998, 34(4): 171—175.

19.   Sun, Y., Wang, E. Z., Huang, Y. Z., The seepage and stability analysis of jointed rock mass slope under the infiltration of rainstorm, Water Resources and Hydropower Technique, 1999, 30(5): 41—45.

20.   Wang, S. S., Chang, H., Tan, J. M., The calculation of groundwater percolation force and stability analysis of slope, Hydrogeology and Engineering Geology, 2003, 2: 41—45.

21.   Chen, J., Yin, J. H., Lee, C. F., Rigid finite element method for upper bound limit analysis of soil slopes subjected to pore water pressure, J. of Engineering Mechanics, ASCE, 2004, 130(8): 886—893.

22.   Wang, Y. J., Xing, J. B., The Discrete Element Method and the Application of It in Geotechnics, Shenyang: Publishing House of Industry College in Northeast of China, 1991.

23.   Wang, H. T., Using the model of crack network percolation coupled with the discrete element method to analyze the stability of high wall slope filling water, Hydrogeology and Engineering Geology, 2000, 2: 30—33.

24.   Jiao, Y. Y., Ge, X. R., Gu, X. R., The simulation of groundwater and anchor rod using with the discrete element method, Journal of Rock Mechanics and Engineering, 1999, 18(1): 6—11.

25.   Ng, C. W. W., Zhan, L. T., Bao, C. G. et al., Performance of an unsaturated expansive soil slope subjected to artificial rainfall infiltration, Geotechnique, 2003, 53(2): 143—157.

26.   Rahardjo, H., Hritzuk, K. J., Leong, E. C. et al., Effectiveness of horizontal drains for slope stability, Engineering Geology, 2003, 69: 295—308.

27.   Iverson, R. M., Reid, M. E., Iverson, N. R., Acute sensitivity of landslide rates to initial soil porosity, 2000, Science, 290(20 October 2000): 513—516.

28.   Harr, R. D., Water flux in soil and subsoil on a steep forested slope. Journal of hydrology, 1997, 33: 159—184.

29.   Lian, Z. Z., The experiment and numerical simulation study on the landside stability under the condition of rockfall and pile load, Master Papers of Chinese Academy of Sciences, 2004, 6: 28—39.

30.   Li, S. H., Lian, Z. H., Wang, J. G, Effect of rock mass structure and block size on the slope stability——Physical modeling and discrete element simulation, Science in China, Series E, 2005, 48(Supp.): 1—17.